

Dislocation thermal resistivity in concentrated alloys*

R. J. Linz,[†] T. K. Chu, A. C. Bouley, F. P. Lipschultz, and P. G. Klemens

Department of Physics and Institute of Materials Science, University of Connecticut, Storrs, Connecticut 06268

(Received 17 January 1974)

The thermal conductivity was measured in the temperature range 0.4 – 4.0 K of concentrated alloys of copper, nickel, and aluminum in both a well-annealed and a heavily deformed state. The alloys are Cu + 10-at.% Al, Cu + 4-at.% Ni, and two commercial alloys, Evanohm and Al-2024. The lattice component of the thermal conductivity was deduced. Strong departures were observed in all cases from the T^2 dependence of the lattice thermal conductivity expected when phonons are scattered only by electrons and by sessile dislocations. With one exception (Evanohm), it was not possible to explain the observed lattice thermal conductivity in terms of nonrandomly arranged sessile dislocations, because the lattice component decreased with increasing T in the range 0.55–0.8 K. It is suggested that the anomaly is due to mobile vibrating dislocations with a resonance frequency. Various resonance models of dislocations are discussed. The magnitude of the lattice thermal conductivity below 0.55 K of the annealed alloys seems to be independent of solute content and consistent with theoretical estimates of phonon-electron scattering.

I. INTRODUCTION

Numerous experiments¹⁻⁹ have shown that the low-temperature lattice thermal conductivity of concentrated alloys does not show the T^2 temperature dependence which is expected from theory.¹⁰⁻¹² Most of these indicate a pronounced change in the temperature dependence near 2–3 K. To explain these results, mechanisms have been invoked involving phonon-electron¹ and phonon-dislocation^{6,8} scattering, though no one model has been entirely successful.

Recently, Ackerman and Klemens¹³ have proposed that the nonrandom orientation of dislocations in dense arrays should cause the lattice thermal conductivity of heavily deformed alloys to depart from a T^2 dependence at a temperature determined by the dislocation density. Well below that temperature, the dislocations should be ineffective in scattering phonons, and the lattice conductivities in the heavily deformed and annealed states should tend to common values. This was predicted to occur below 1 K in typical cases.

The measurements described in this paper were made in an effort to test the predictions of the Ackerman-Klemens model. We shall find that our results are qualitatively consistent with this model, but that the occurrence of an additional scattering mechanism makes a detailed comparison impossible. This additional mechanism needed to explain the present results seems to be associated with mobile dislocations.

II. EXPERIMENTAL PROCEDURE

A. Specimen preparation

Thermal and electrical conductivity measurements were made on specimens of copper containing 10-at.% aluminum, copper containing 4-at.%

nickel, Evanohm¹⁴ (71-at.% Ni, 21-at.% Cr, 5-at.% Al, 2-at.% Cu, approximately), and a commercial aluminum alloy, ASTM No. 2024 (96-at.% Al, 1.9-at.% Cu, 1.7-at.% Mg, and 0.2-at.% Mn, approximately). Hereafter, we will refer to these alloys as Cu-10-at.%-Al, Cu-4-at.%-Ni, Evanohm, and Al-2024, respectively. All specimens were polycrystalline rods of circular cross-section and were measured in either a highly annealed or heavily deformed state. The history, geometry and residual resistivity of the seven specimens are given in Table I.

The copper alloys were obtained from the supplier¹⁵ in the form of rods. They had been prepared from 99.999% pure copper and aluminum, and 99.99% pure nickel. The Cu-10-at.%-Al alloy was from the same batch as that measured in Ref. 3. The Evanohm specimen was donated by the manufacturer in the form of a 0.64-cm-nominal-diam hot-rolled rod. The Al-2024 alloy was laboratory stock in the form of a 0.64-cm-diam rod.

All alloys were deformed by swaging at room temperature at this laboratory, with the exception of Cu-10-at.%-Al, which was swaged by the supplier. The final specimen diameters were 0.32 cm for Cu-10-at.%-Al, Cu-4-at.%-Ni, and Al-2024, and 0.48 cm for Evanohm. Attempts to further swage the Evanohm rod down to a 0.32-cm diameter resulted in macroscopic cracking and pitting, and made that specimen unsuitable. It may be assumed that the swaging process resulted in all cases in extremely dense dislocation arrays, with a saturation dislocation density N_d in excess of 10^{11} lines/cm².

In addition to measurements in the deformed state, we measured specimens in the annealed state. These specimens were companion samples, which had undergone the same deformation pro-

TABLE I. Sample characteristics, geometry, and residual resistivity ρ_0 .

Sample composition	Physical state	Grain size (mm)	Diameter (in.)	Length L (in.)	ρ_0 ($\mu\Omega$ cm)
(a) Cu-10-at. %-Al	Cold swaged, 1-in. to $\frac{1}{8}$ -in. diam.	$\leq 0.01-0.1$	0.1251	2.00	8.03
(b) Cu-10-at. %-Al	As (a), then annealed at. 1060 °C for 60 h	2-4	0.1257	2.00	7.323
(c) Cu-4-at. %-Ni	Cold swaged, 1-in. to $\frac{1}{8}$ -in. diameter	0.1	0.1236	2.00	4.540
(d) Cu-4-at. %-Ni	As (c), then annealed at. 1090 °C for 60 h	2-6	0.1240	2.00	4.920
(e) Evanohm	As received (hot rolled)	...	0.3276	2.00	122.8
(f) Evanohm	As (e), then cold swaged, $\frac{5}{16}$ - to $\frac{3}{16}$ -in. diameter	...	0.1775	2.00	113.4
(g) Al-2024	Cold swaged, $\frac{1}{4}$ - to $\frac{1}{8}$ -in. diameter (etched).	...	0.115	2.00	3.157

cess, and were, in fact, cut from the same rod, but which were subsequently annealed to within 20 °C of their melting temperature for 60 h. This is expected to remove most dislocations, with residual dislocation densities expected^{16,17} to be no greater than 10^7 cm⁻². This annealing produced marked recrystallization, with grain sizes growing from roughly less than 0.1 mm to 3-5 mm.

The Evanohm specimen was measured in the well annealed state only in the range 1-4 K. In that range the results coincided with those of the "as-received" or hot-rolled specimen, the lattice thermal conductivities differing only by 3% and showing the same temperature dependence. We therefore regard the hot-rolled specimen as equivalent to a well-annealed specimen, and the data for the well-annealed state is actually derived from measurements made on the hot-rolled specimen.

B. Measurements

The copper alloys were measured first in the heavily deformed and then in the well annealed state. Evanohm was measured first in the as-received and then in the deformed state, while Al-2024 was measured in the deformed state only.

Thermal conductivities were measured using a standard steady-state technique. The specimen, of cross-sectional area A , is mounted with one end thermally anchored to a liquid bath maintained at constant temperature. Heater power Q is applied at the other end, and establishes a difference of temperature ΔT between two thermometers sepa-

rated by a distance L . The thermal conductivity K is given by

$$K = (\dot{Q}/\Delta T) L/A .$$

The apparatus and measuring techniques in the 1-4-K range¹⁸ and the 4-77-K range^{19,20} have been adequately described. For measurements below about 1.3 K, a commercial ³He refrigerator²¹ was used, and temperatures were determined both by carbon and by germanium resistance thermometry. The germanium resistors were calibrated against the vapor pressure of ³He; the carbon resistors were calibrated during each thermal conductivity run against the germanium resistors. Complete details of all apparatus and thermometry used below 1.3 K are described elsewhere.²²

To check the consistency of measurements below 1.3 K, the thermal conductivity of an annealed pure-copper rod was measured. Its thermal conductivity should be due entirely to the electronic component K_e , and obey the Wiedemann-Franz law, so that

$$K = K_e = L_0 T / \rho_0 .$$

Here L_0 is the "ideal" Lorenz number, 2.445×10^{-8} W Ω K², and ρ_0 is the residual electrical resistivity. The quantity $K\rho_0/T$ was found to be within 0.5% of 2.32×10^{-8} W Ω K² from 0.5 to 1.3 K. The discrepancy between this value and L_0 is due to an uncertainty of $\sim 10\%$ in the determination of ρ_0 (16 ± 2 n Ω cm).

The absolute accuracy of the thermal conductiv-

ity measurements reported in this work is estimated to be within 1%; errors are chiefly due to uncertainties in measured specimen geometry. Precision of the measurements, as may be seen from the scatter in the data, is usually within 0.5%. To minimize the effect of errors due to geometry on the lattice thermal conductivity, the thermometer clamps were also used as potential probes during the electrical resistivity measurements. The clamps were not moved until all the electrical and thermal measurements on each specimen were completed. In the annealed and deformed samples, equal separation between the clamps was reestablished to within 0.1% by means of a precision-machined mounting jig. Random errors in the thermal conductance $\dot{Q}/\Delta T$ are mainly due to small temperature fluctuations of the liquid bath and to thermometry errors.

The thermal conductivities in the ^3He cryostat were measured on two specimens at a time. The specimen pairs were: Cu-10-at. %-Al, annealed and Evanohm, hot-rolled; Cu-10-at. %-Al, swaged and Al-2024; Cu-10-at. %-Al, elongated 12% (no data are reported for this sample, owing to a poor thermometer contact) and Evanohm, swaged; Cu-4-at. %-Ni, annealed and Cu-4-at. %-Ni swaged. Germanium thermometers were placed on that specimen which had the lesser lattice thermal conductivity. Carbon thermometers, placed on the other specimen, were calibrated against the germanium thermometers under condition of zero heater current. The specimen pairs were chosen, as far as possible, to have equal thermal conductances. Thus any systematic errors would show up equally strongly in the data for each specimen, and would be readily identified and eliminated. The conductances were nearly identical for the first and for the last pairs. In the worst match, the conductance of swaged Al-2024 was nearly twice that of swaged Cu-10-at. %-Al. Heater resistances were matched to the specimens in such a way that, for the same heater current, the specimen heaters would be at the same temperature. The heaters were in series and electrically connected but thermally insulated by Evanohm wire leads of 25-cm length and 6.4×10^{-3} -cm (0.0025-in.) diameter. For typical heater powers, $\dot{Q} \approx 1 \mu\text{W}$, maximum heat leaks from one heater to the other are estimated²³ to be no larger than $10^{-4}\dot{Q}$, even assuming an extreme difference of 1 K in heater temperature.

Electrical resistivities of all specimens were measured from 1.2 to 4.2 K with instrumentation and techniques essentially as described by Burckbuchler and Reynolds.²⁴ In Table I, ρ_0 is taken to be the resistivity at 1.2 K. The Cu-10-at. %-Al specimen had a resistivity which increased slightly (by about 0.06%) from 4 to 1.2

K. This may be due to trace amounts of iron introduced in the swaging process.³ The resistivity of the Evanohm specimens increased by nearly 0.3% from 4 to 1.2 K, in agreement with previously reported data on fine wires of this alloy.²⁵ The resistivities of Cu-4-at. %-Ni and Al-2024 were found to be constant in this temperature range. The electrical resistivities were not measured below 1 K, and were approximated by linear extrapolation from higher temperatures except for Evanohm, where previous data²⁵ were available.

The electrical resistivities of Cu-4-at. %-Ni and of Evanohm were higher in the annealed than in the deformed state, as commonly observed for alloys containing transition metals.²⁶ We are not aware of any general explanation for this behavior. However, for the case of copper-nickel, this may be a consequence of a tendency to form clusters.²⁷

C. Data analysis

The measured thermal conductivity is the sum of an electronic component K_e and a lattice component K_g , i. e.,

$$K = K_e + K_g . \quad (3)$$

From Eq. (1) and (2) the lattice conductivity can be obtained by means of

$$K_g = [(\dot{Q}/\Delta T) - L_0 T/R](L/A) , \quad (4)$$

where R is the residual electrical resistance of the specimen. If $K_g = BT^2$, as predicted by standard theory at very low temperatures,¹⁰⁻¹² then

$$K/T = L_0/\rho_0 + BT . \quad (5)$$

Thus, in a plot of K/T vs T , the data points should fall on a single straight line of slope B and intercept L/ρ_0 . If K_g is obtained from (4) and $\log_{10} K_g$ is plotted against $\log_{10} T$, the low-temperature data points should lie on a single straight line of slope 2. Any departure from the $K_g \propto T^2$ dependence should be clearly evident on either plot.

III. RESULTS

In Figs. 1-4, graphs are presented of K/T vs T for all specimens. In Figs. 5-7, K_g as deduced from Eq. (4) is shown as a function of T on a log-log scale for the same specimens except Al-2024, for which K_g is too small to be deduced with confidence (see Fig. 4). Below 1 K, the data points are so dense when plotted on a linear temperature scale that only some representative points can be shown on the graph of K/T vs T .

The values of K/T for all specimens depart markedly from the linear behavior of Eq. (5). Except for Al-2024, these departures indicate that K_g departs from a T^2 variation. If these departures from a straight-line behavior of K/T were the re-

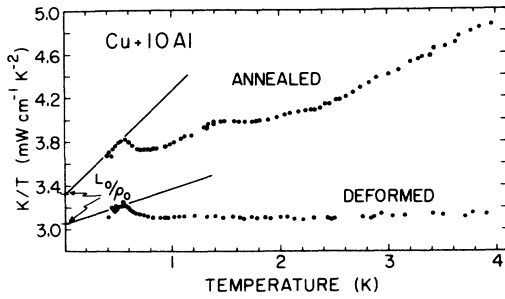


FIG. 1. K/T vs T for Cu-10-at.-%-Al. Solid lines through L_0/ρ_0 indicate $K_g \propto T^2$.

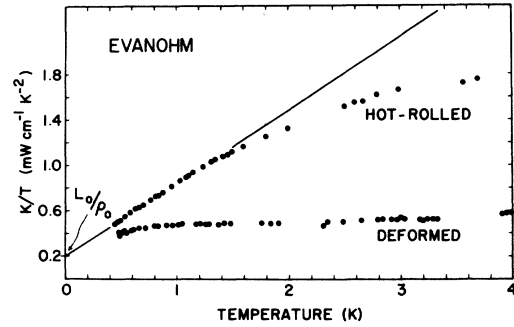


FIG. 3. K/T vs T for Evanohm. Solid line through L_0/ρ_0 indicates $K_g \propto T^2$.

sults of irregularities in K_g , corresponding changes should also occur in the electrical resistivities. The slight changes in electrical resistivity observed in some specimens in the range 1.2-4 K could not account for changes in the thermal conductivity of the observed magnitude. Although we did not measure the electrical resistivity of the copper alloys below 1 K, Rowlands *et al.*⁹ found the resistivity of their Cu-10-at.-%-Al specimen to be constant below 1 K, while their thermal-conductivity data on that alloy is similar to ours. It is thus unlikely that the resistivity of our alloys departs significantly from being constant below 1 K, and since it is unlikely that the Wiedemann-Franz law is invalid below 1 K, the observed departures of K/T from a linear dependence on T most probably arise from the behavior of the lattice component rather than the electronic component.

We present the lattice thermal conductivity results both in the form of plots of K/T vs T (Figs. 1-4) and also in the form of plots of K_g vs T (Figs. 5-7), as certain features of the data are illustrated more clearly on one type of plot than the other. Thus, the pronounced change in slope near 2.5 K of the K/T curve of the annealed copper alloys (Figs. 1

and 2) is barely discernible on the logarithmic plot of K_g . Again, in the deformed Cu-10-at.-%-Al, there is a rapid variation in the temperature dependence of K_g (Fig. 5) near 2.5 K which is almost totally obscured in the K/T -vs- T plot (Fig. 1).

The occurrence of the peak near 0.55 K, which is common to all copper alloy specimens, has been verified through numerous cross checks of thermometry and measuring techniques. Figure 4 compares data for Cu-10-at.-%-Al with hot-rolled

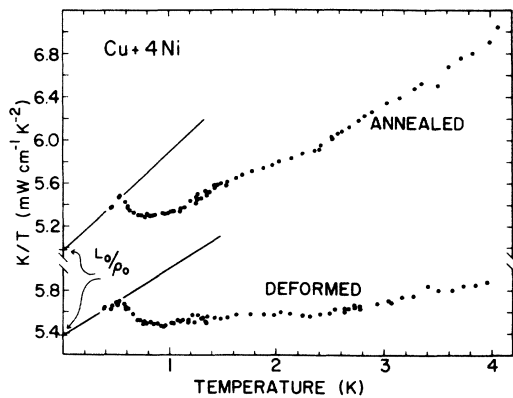


FIG. 2. K/T vs T for Cu-4-at.-%-Ni. Solid lines through L_0/ρ_0 indicate $K_g \propto T^2$.

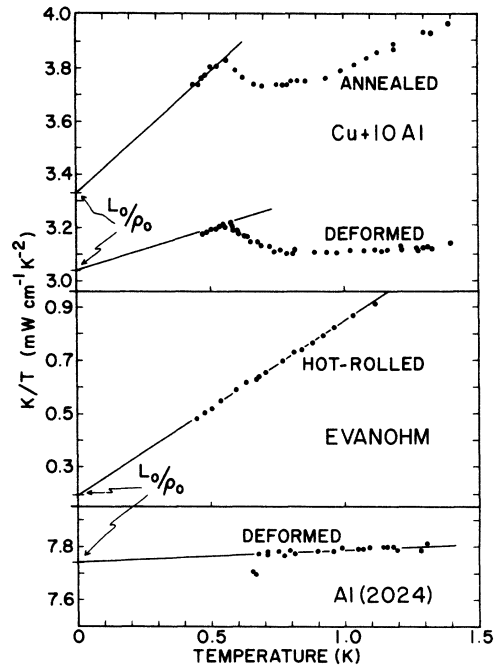


FIG. 4. K/T vs T for some alloys below 1 K. Results for Evanohm and Al-2024 were obtained by carbon thermometry, which was based on the germanium thermometers on the Cu-10-at.-%-Al samples during a thermal-conductivity run. The dashed line for Al-2024 represents 20 or so data points, and is indicative of superconducting transition.

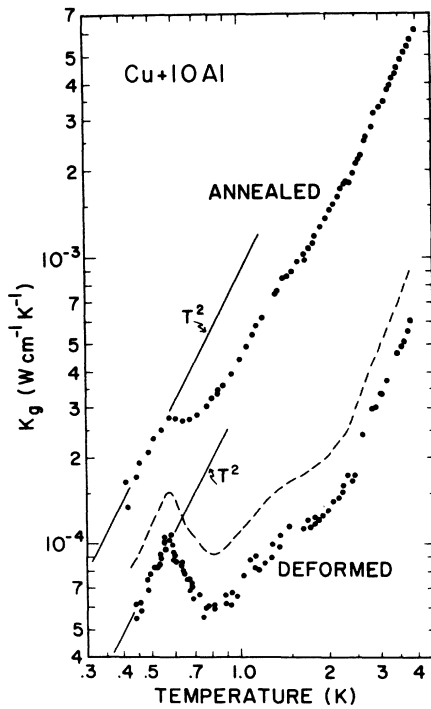


FIG. 5. K_g vs T for Cu-10-at.-%-Al. Solid lines indicate $K_g \propto T^2$. Dashed line represents K_g increased by a factor of 1.5, denoting the hypothetical lattice thermal conductivity for "bare" dislocations.

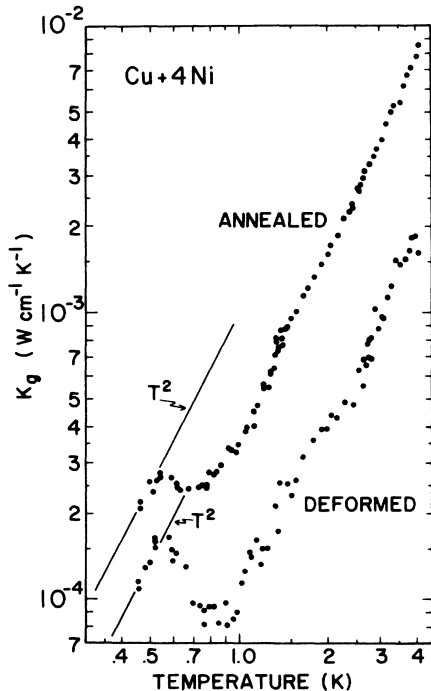


FIG. 6. K_g vs T for Cu-4-at.-%-Ni. Solid lines indicate $K_g \propto T^2$.

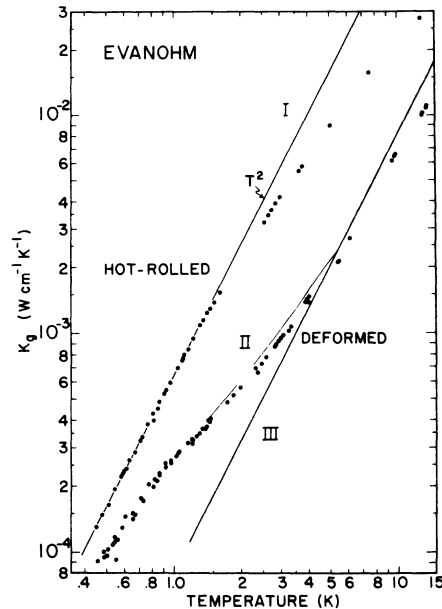


FIG. 7. K_g vs T for Evanohm. Curve I: K_g as limited by electron-phonon scattering only. Curve II: K_g for deformed state with nonrandomly oriented dislocations. Curve III: K_g for a deformed state with randomly oriented dislocations.

Evanohm and Al-2024 in the region of the peaks. If the peaks in the copper alloys were due to any systematic error, corresponding features should appear in Evanohm and Al-2024, since the thermometers of these two specimens were calibrated below 1 K against the thermometers of the Cu-10-at.-%-Al specimen, and since all these specimens had similar conductances.

The salient features of the lattice thermal conductivity of the copper alloys is (a) a pronounced change in slope near 2.5 K and (b) a peak in the lattice thermal conductivity near 0.55 K. These results are consistent with previous measurements on noble metal alloys. Thus, in the 1-4-K range, a change in the slope of K/T has been observed quite often,^{1,3-9,28} and needs no longer to be regarded as unusual. The temperature of the break in slope varies from about 2 to 3.5 K. Below 1 K, Rowlands *et al.*,⁹ have also observed a "bump" in their K/T plot for Cu-10-at.-%-Al, which is similar to ours and may thus correspond to a "peak" in the K_g curve. The same group more recently²⁸ reported such bumps in a silver alloy and in gold and copper alloys. The earlier measurements of Jericho²⁹ on silver alloys indicate a peak in K_g at somewhat higher temperatures than our peak, also followed by a rapid decrease with decreasing temperature.

The thermal conductivity of deformed Al-2024

should be explained differently. The thermal conductivity fits Eq. (5) about 0.65 K; below that temperature K/T drops rapidly below the curve of Eq. (5). Presumably the alloy is then in the superconducting state. The apparent transition temperature of 0.65 K differs markedly from that of pure aluminum (1.2 K). This may be partly due to alloying. However, thermal-conductivity data cannot be used to determine a transition temperature by graphical means, particularly when the transition is not a simple one, as is likely to be the case in this alloy.

IV. THEORY

A. Scattering of phonons by electrons and sessile dislocations

The important resistive mechanisms limiting the lattice thermal conductivity at low temperatures are scattering of phonons by conduction electrons and by dislocations. Both scattering processes yield a lattice thermal resistivity varying inversely as T^2 , i. e.,

$$W_g = 1/K_g = W_{ge} + W_{gd}, \quad (6)$$

where W_{ge} and W_{gd} are the resistivities due to electrons and dislocations, respectively.

According to standard theory,

$$W_{ge} = GT^{-2}, \quad T \ll \Theta, \quad (7)$$

where Θ is the Debye temperature. The parameter G can be estimated from the intrinsic electronic conduction properties, preferably from the ideal electronic thermal conductivity at low temperatures.³⁰ On the assumption that the electrons interact equally strongly with phonons of all polarizations, the values of G are as follows^{11,30}:

$$\begin{aligned} G &\simeq 710 \text{ W}^{-1} \text{ cm K}^3 \text{ for Cu} \\ &\simeq 430 \text{ W}^{-1} \text{ cm K}^3 \text{ for Ag} \\ &\simeq 350 \text{ W}^{-1} \text{ cm K}^3 \text{ for Au.} \end{aligned} \quad (8)$$

The theory leading to (7) assumes that the phonon wavelength λ is less than L_e , the mean free path of the important electrons, otherwise W_{ge} is reduced by a factor of order L_e/λ . Since $\lambda \propto 1/T$ for the dominant phonons, this modification would lead to $W_{ge} \propto 1/T$, as pointed out by Pippard.³¹

Scattering of phonons by sessile dislocations arises mainly from the long-range strain field around each dislocation. For a single dislocation $W_{gd} \propto T^{-2}$. For a random assembly, the same dependence should hold, and W_{gd} should be proportional to the dislocation density N_d . A recent estimate³² gives for copper

$$W_{gd} T^2 \simeq 3.2 \times 10^{-8} N_d \text{ W}^{-1} \text{ cm K}^3. \quad (9)$$

Comparing (8) and (9) we see that about 2×10^{10} dislocations per cm^2 are required to make W_{gd} equal to W_{ge} .

This theory assumes that the strain field around each dislocation, falling off inversely with distance from the center, extends to infinity. One would, however, expect dislocations to interact with each other and to be arranged such that the long-range strain energy is minimized. This would reduce the long-range strain field and thus the scattering of long-wavelength phonons. One such arrangement is that of dislocation dipoles; phonon scattering by dislocation dipoles has been treated by Grüner and Bross.³³ Another model, less specific, assumes that the strain field is truncated at a distance R comparable to the average distance between dislocations.¹³ Both models have a critical wavelength and frequency, and hence a critical temperature. For phonons of lower than critical frequency the scattering drops rapidly. In the model of Ackerman and Klemens the critical wavelength is determined by the dislocation density; in the model of Grüner and Bross it is determined by the dipole spacing. Since the dipole spacing must be less than the average interdislocation distance if the dipole model is to be meaningful, the dipole model has a higher critical temperature. Otherwise, both models are similar and it may be hard to distinguish between them from thermal-conductivity data alone.

Another common feature of these two models is that the scattering of low-frequency phonons (below the critical frequency) is so weak that the thermal conductivity integral would diverge unless another scattering process is invoked to remove the divergence. Grüner and Bross invoke anharmonic three-phonon processes conserving momentum (N processes). This may be an appropriate choice in insulators at higher temperatures. In alloys, particularly at very low temperatures, the dominant process removing the low-frequency divergence is much more likely to be the scattering of phonons by electrons, and this latter process was incorporated into the theory of Ackerman and Klemens.

The model of Ackerman and Klemens¹³ results in the following behavior of K_g : at high temperatures and at low temperatures, $W_g \propto 1/T^2$; but at high temperatures, $W_g = W_{ge} + W_{gd}$, while at low temperatures $W_g = W_{ge}$, with W_{ge} and W_{gd} as given in (7) and (9). The transition from the high- to the low-temperature regime occurs around a critical temperature T_c . That temperature T_c varies inversely as the cutoff radius R and is thus proportional to $N_d^{1/2}$; it enters as a parameter in the theory. Another parameter is the ratio W_{gd}/W_{ge} , which affects the shape of the curve in the intermediate region, but is of course also a function of N_d . For a typical dislocation density of about 10^{11}

cm^{-2} , W_{ϵ} is midway between $W_{\epsilon e}$ and $W_{\epsilon e} + W_{\epsilon d}$ at a temperature near 1 K.

B. Need to invoke other interactions

The behavior predicted by Ackerman and Klemens¹³ is seen in the case of Evanohm (Fig. 7). The copper alloys, however, show a markedly different temperature dependence; the thermal conductivity is not a monotonically increasing function of temperature, but shows a minimum around 0.7 K and a small maximum at about 0.55 K. Hence, while the effect discussed by Ackerman and Klemens may be present, there must also be an additional interaction.

Scattering of phonons by electrons and scattering by sessile dislocations of any spatial distribution result in a phonon mean free path which is a function of frequency, but not of temperature. No matter what the frequency dependence of the mean free path, the temperature dependence of the resulting thermal conductivity must be such that the conductivity increases with temperature or is at most constant over some temperature range. It is not possible, however, to have the conductivity decrease with increasing temperature, unless one invokes a mean free path which is intrinsically temperature dependent and which decreases with increasing temperature. Thus, to explain the minimum in K_{ϵ} around 0.7 K one must invoke a scattering process which is intrinsically temperature dependent.

One such process is the anharmonic three-phonon interaction, which is responsible for the down turn in K_{ϵ} above about 30 K in copper alloys. Because the three-phonon relaxation rate decreases rapidly with decreasing temperature, it would be difficult to construct a model where these interactions are important below 1 K, even though N processes would be somewhat stronger than U processes. In such a model one would have a small group of phonons which are only weakly scattered by electrons and dislocations, and which are brought into thermal equilibrium by N processes. This is indeed the role of the N processes in the model of Grüner and Bross,³³ where low-frequency phonons are only very weakly scattered by dislocation dipoles. Their theory does, in fact, lead to a minimum in K_{ϵ} under some conditions. However, this is not likely to explain a minimum below 1 K, since the relaxation time for N processes of the dominant thermal phonons varies inversely as T^5 . In order to have a minimum in K_{ϵ} below 1 K, it would be necessary to have a small group of phonons with a very long mean free path. Since that mean free path would have to be much larger than the grain size, such a model is highly implausible.

C. Resonance scattering of phonons by vibrating dislocations

The anomalous temperature dependence of K_{ϵ} below 0.7 K is seen in all samples except Evanohm, both in the deformed and the annealed state. However, the anomaly is relatively smaller in the annealed specimens, so that it seems plausible to ascribe it to dislocations. Also, since sessile dislocations cannot account for the anomalous temperature dependence, the anomaly must be due to the motion of dislocations under the stress of the thermal phonons. Mobile or fluttering dislocations will scatter phonons much more strongly than sessile dislocations. Even the relatively small number of dislocations in annealed specimens might cause an appreciable reduction of K_{ϵ} if they are mobile, but not if they are immobile.

The strong scattering of phonons by mobile dislocations is well established by theory^{34,35} as well as by observations.^{8,36-38} Owing to the stress of an incident lattice wave the dislocation is displaced, and the time-varying displacement radiates phonons. Also, the dislocation responds to the impressed stress field like a forced oscillator having a natural resonance frequency ω_0 . The response of the dislocation to the applied stress, and thus the rate at which energy is extracted from an incident lattice wave, are greatest for frequencies near the resonance frequency.

A resonance scattering model would thus not only explain strong scattering by dislocations, but would also lead to a thermal resistance which is particularly pronounced at temperatures around $\hbar\omega_0/k$, where k is the Boltzmann constant and \hbar the rationalized Planck constant. However, if resonance scattering were just a function of frequency its effect on the thermal conductivity curve would be an inflection, not a minimum. A minimum can only result from a temperature-dependent resonance of the scattering.

In the absence of a detailed theory we cannot fully explain the observed thermal conductivity curves. In the following discussion we shall concentrate on information which bears on the resonance frequency ω_0 .

Kusunoki and Suzuki,⁸ who observed departures from the T^2 dependence of K_{ϵ} near 3 K in deformed Cu-15-at.-%-Al and attributed this to resonance scattering, proposed that the dislocations are dissociated with each partial dislocation vibrating independently from the other. The restoring force is attributed to binding by solute atmospheres (Cottrell locking) and they relate the resonance frequency to flow stress. Their model is thus not sensitive to the detailed locking mechanism. In Cu-15%-Al one would, for example, expect the stacking fault between the two partial dislocations to be stabilized by a thin layer of hexagonal-phase

aluminum-rich material (Suzuki locking), and the resonance could also be associated with the vibration of each partial dislocation relative to the edge of the solute-rich plane. In either case one would expect this resonance to occur only in high-concentration alloys, preferably near the boundary of the α phase.

A similar but somewhat more general model has been treated by Kronmüller.³⁹ A pair of partial dislocations are separated by a stacking-fault ribbon, the equilibrium separation being determined by the stacking-fault energy. The two partials vibrate relative to each other. The resonance frequency is proportional to Γ , the stacking-fault energy per unit area, and is given by

$$\omega_0 = \Gamma (2/k_0 M_{\text{eff}})^{1/2}, \quad (10)$$

where M_{eff} is an effective dislocation mass and the constant k_0 depends on the elastic moduli and the type of dislocations. Usually, Γ is much more sensitive to solute concentration than are the other parameters. Typically, ω_0 is of the order of 10^{11} sec⁻¹. Significantly, there should be two resonance frequencies, corresponding to screw and to edge dislocations, with the former frequency higher by a factor of roughly 2.

A different resonance model is that of Granato and Lücke,³⁵ where the dislocations vibrate like a string stretched between two pinning points. If L is the length of a free dislocation segment, the resonance frequency is

$$\omega_0 \simeq 2\pi v/3L, \quad (11)$$

where v is the transverse sound velocity. In a random network of dislocations of density N_d , $N_d \simeq 1/L^2$. The length L is also comparable to the critical cutoff radius R in the theory of Ackerman and Klemens.¹³ Resonance scattering according to the string model should then be important at about the same temperature where the nonrandom array of sessile dislocations would cause K_L to depart from a T^2 dependence.

Finally, there is the resonance frequency which is characteristic of the Peierls potential. This potential separates one stable dislocation position from the adjacent position in the lattice,⁴⁰ and it is possible for the dislocation to vibrate in the potential trough formed by this potential. Interestingly, there are two different potentials, or stresses needed to move a dislocation, one for edge and one for screw dislocations. Since the Peierls stresses in fcc metals differ by roughly a factor of 10 for these two dislocation types, one would expect the resonance frequencies to differ roughly by a factor of 3.

The thermal vibrations of dislocations have an amplitude small compared to the interatomic dis-

tance. The displacement of a dislocation line must be understood to be a small displacement of many atoms around the dislocation, but forming a coherent displacement pattern. This is in contrast to the vibration of a dislocation line under the influence of an ultrasonic wave, where the displacement of the line is over distances larger than the interatomic distance, so that the motion of individual atoms is of the order of an interatomic distance, and where dislocations can break away from obstacles.

V. DISCUSSION

The lattice thermal conductivities of the deformed and annealed alloys depart markedly from the $K_L \propto T^2$ variation expected from scattering of phonons by electrons and by random sessile dislocations. On a plot of K_L/T vs T , these departures appear as a gradual transition from one limiting slope (or value of K_L/T^2) to another (see Figs. 1-3). These results resemble those of Kapoor *et al.*²⁸ However, on a plot of K_L vs T (see Figs. 5-8) one sees that, except for Evanohm, the lattice component K_L does not increase monotonically with increasing T , but passes through a maximum, followed by a minimum. These maxima and minima occur in the annealed as well as in the deformed copper alloys. Furthermore, K_L increases faster than T^2 in the range 3-4 K.

To explain this, phonon resonance scattering associated with vibrating dislocations is invoked. The occurrence of the minimum in the annealed copper alloys is attributed to residual dislocations, which are not removed by annealing. Since this residual dislocation density must be much smaller than the density of dislocations in the deformed specimens, the residual dislocations must scatter phonons much more strongly than sessile dislocations.

The absence of a minimum in K_L of Evanohm implies either that the dislocations in this material are not mobile, or that their vibrations are heavily damped.

The value of K_L/T^2 of the two annealed copper alloys at the lowest temperatures appears to be limited by phonon-electron scattering and is in rough quantitative agreement with theory [Eq. (8)].

A. Evanohm

The lattice thermal conductivity of Evanohm (Fig. 7) exhibits the behavior expected from the theory of Ackerman and Klemens¹³ for dense non-random dislocation arrays. The hot-rolled sample shows the $K_L \propto T^2$ variation expected for phonons scattered by electrons and possibly by residual dislocations. The gradual drop of K_L below the T^2

curve (curve I) above 2 K is probably due to phonon scattering by solute atoms. The high solute concentration makes this strong scattering quite plausible; however, we have not attempted to explain this scattering quantitatively.

Except for the same solute atom scattering, the deformed alloy would follow a $K_f \propto T^2$ variation above about 5 K, indicated by curve III. The additional dislocation density introduced by deformation is estimated, from Eq. (9), which also applies to nickel alloys, to be about 3.3×10^{11} lines/cm².

At lower temperatures, the K_f curve of the deformed specimen approaches that of the hot-rolled specimen, but does not merge into it. It thus appears that not all dislocations have their long-range strain field "truncated," but that a small fraction (about 7%) of the newly introduced dislocations act as isolated dislocations.

The $K_f(T)$ curve in the transition region (curve II) is similar to the theoretical curves of Ackerman and Klemens¹³ for Cu-10-at.-%Al. These authors give curves for the cases when $W_{gd}/W_{ge} \approx 1$ at high temperatures and when $W_{gd}/W_{ge} \approx 3$. For the present purposes W_{ge} is the thermal resistivity of the hot-rolled specimen; it may include a contribution from residual isolated dislocations which would play the same role as W_{ge} in that theory, so that these resistive mechanisms may be combined. In the present case, $W_{gd}/W_{ge} \approx 7$. As the dislocation density increases, the range of the truncated strain field becomes shorter, and the temperature where departures from $K_f \propto T^2$ should become apparent becomes higher. If T_c is the temperature at which K_f is 50% above curve III, and if one extrapolates T_c linearly as a function of W_{gd}/W_{ge} from the values given in Ref. 13, one would expect T_c to be about 1.8 K for Cu-10-at.-%Al when W_{gd}/W_{ge} is 7. This must be multiplied by a factor 1.4 to account for the higher Debye temperature of Evanohm, so that the expected value of T_c in the present case is about 2.5 K. From Fig. 7 it is seen that $K_f(T)$ lies above curve III by a factor of 1.5 at about 2.8 K. Thus, curve III not only resembles the theoretical curves of Ref. 13 in general shape, but there is a rough agreement with respect to the temperature at which the departures from $K_f \propto T^2$ occur. This latter agreement indicates that the truncated strain field model is a better description than the dislocation dipole model for phonon scattering.

Since Evanohm does not show the minimum in K_f seen in the other alloys, it would appear that resonance scattering is either absent or considerably modified. Either the dislocations are immobile, owing to the high concentration of solute atoms, or the dislocation motion is highly damped, so that the amplitude of vibration and the consequent phonon scattering is greatly reduced.

B. Mobile dislocations

In deformed Cu-10-at.-%Al and Cu-4-at.-%Ni there also is an increase in K_f/T^2 as one goes to lower temperatures. However, K_f increases with decreasing temperature between 0.8 and 0.55 K, so that the scattering of phonons is not just frequency dependent and cannot be entirely due to sessile dislocations; there must also be resonant phonon scattering. The major reduction in K_f on plastic deformation must still be attributed to sessile dislocations. It is quite likely that these dislocations are arranged not at random but so as to truncate the long-range strain fields of most of them, as postulated in Ref. 13 since the value of K_f/T^2 of the two deformed copper alloys below 0.55 K is only a factor of 2 below that of the annealed specimens, and substantially higher than K_f/T^2 at 4 K. However, the presence of the additional scattering mechanism makes it impossible to compare the data with theory.

From Eq. (9) and the thermal resistivities at 3 K, the density of sessile dislocations introduced by swaging is estimated to be 1.5×10^{11} lines/cm² for Cu-4-at.-%Ni and 6.6×10^{11} lines/cm² for Cu-10-at.-%Al.

The latter estimate must be corrected for the fact that in Cu-10%-Al scattering of phonons by dislocations is probably enhanced by solute atmospheres around each dislocation.⁴¹ Mitchell *et al.*³ estimated, from annealing studies on a similar alloy, that solute atmospheres increase the dislocation resistance by a factor of about 1.5 over that for "bare" dislocations. This factor would reduce the dislocation density estimate in the deformed Cu-10-at.-%Al specimen to about 4.5×10^{11} lines/cm². For Cu-4-at.-%Ni, where the atomic misfit and the mass difference between solvent and solute atoms is small, one would not expect an important enhancement of dislocation scattering by solute atmospheres.

Even this reduced estimate of the dislocation densities in deformed Cu-10-at.-%Al may be too high, because some of the additional thermal resistivity at 3 K in the deformed sample may be due to mobile dislocations. In the absence of a complete theory of scattering by mobile dislocations, this contribution cannot be evaluated. However, the higher the temperature, the greater should be the effect of sessile dislocations relative to the mobile dislocations, provided the resonance frequency is low. Since most deformed alloys follow roughly a $K_f \propto T^2$ dependence above 4 K until point defect and anharmonic effects become important, these values of W_{gd} are not violently in error.

It is interesting that the major resonant frequency seems the same in both Cu-10-at.-%Al and Cu-4-at.-%Ni, and in both deformed and annealed

specimens, since the minimum in K_g is at about 0.7 K in all these cases. This argues against the vibrating string model³⁵ and against the model of vibrations of dissociated dislocations.^{8,39}

In the vibrating string model one would expect the average loop length to vary inversely as the square root of the dislocation density. Since the dislocation density in the annealed specimens should be much lower than in the deformed specimens, one would have expected the resonance frequency in the annealed specimens to be shifted down by an order of magnitude. This shift clearly does not occur, so that the only way in which one could reconcile the present observations with that model would be to assume that while the average dislocation density is lowered in the annealed specimens, the mobile dislocations occur in regions where the dislocation density is high, and comparable to the density in deformed specimens. This seems unlikely.

The resonance frequency seems the same in both Cu-10-at.-%-Al and Cu-4-at.-%-Ni, even though their stacking fault energies differ by an order of magnitude.^{42,43} This seems to rule out a resonance mechanism based on vibrating stacking faults, since that theory³⁹ predicts the resonance frequencies to be proportional to the stacking fault energies. This model does have the attractive feature of predicting two resonance frequencies; our data indicate a small inflection around 2 K besides the major minimum at about 0.7 K. However, two resonance frequencies are a consequence of the presence of edge and screw dislocations, and may thus be common to many models. They also appear in the Peierls potential vibration model. The insensitivity of the position of the resonance to alloy composition and to the state of deformation thus tends to favor the Peierls potential as the source of the restoring force in a resonance model of vibrating dislocations.

It may be reasonable to identify the stronger resonance at 0.7 K with edge dislocations and the weaker resonance near 2.5 K with screw dislocations. Not only is the Peierls potential stronger for screw dislocations than for edge dislocations,⁴⁰ so that the former should give a higher resonance frequency, but edge dislocations are known to be the predominant type in deformed Cu-Al alloys,⁴⁴ so that in the deformed alloys the resonance at lower frequency should be the stronger one, as is indeed the case.

It is still necessary to explain why there is visible resonance scattering in the annealed alloys, even though the dislocation density must be smaller by a factor of at least 100. On an additive resistance approximation the resonance scattering in the annealed alloys relative to the deformed alloys is reduced by a much smaller factor (about 5 in Cu-

10-at.-%-Al, even less in Cu-4-at.-%-Ni). One would have to assume that annealing greatly reduces the density of sessile dislocations, but changes the density of mobile dislocations by a much smaller amount. A much more attractive alternative would be to assume that the vibrating dislocations scatter some phonons very strongly, but leave other phonon groups unaffected. The effect of resonance scattering on the thermal conductivity would then saturate as a function of the density of mobile dislocations, and the saturation reduction would always be the same fractional reduction in K_g at resonance. The present observations are not inconsistent with such a model. Furthermore, this is the same argument that Anderson and Malinowski³⁸ used to interpret the effect of vibrating dislocations on the thermal conductivity of lithium fluoride. In their case it was phonons of one polarization branch which were preferentially scattered. It is also possible that the group of phonons which are strongly scattered could belong to some range of frequencies.

C. Phonon-electron scattering

In the annealed as well as the deformed specimens of Cu-10-at.-%-Al and Cu-4-at.-%-Ni, the lattice conductivity drops off rapidly as T is decreased below 0.55 K. The temperature range available is too narrow to determine the temperature dependence of K_g below the secondary maximum, but the experimental values are not inconsistent with a $K_g \propto T^2$ variation. The lattice conductivity of the two annealed specimens are inter-

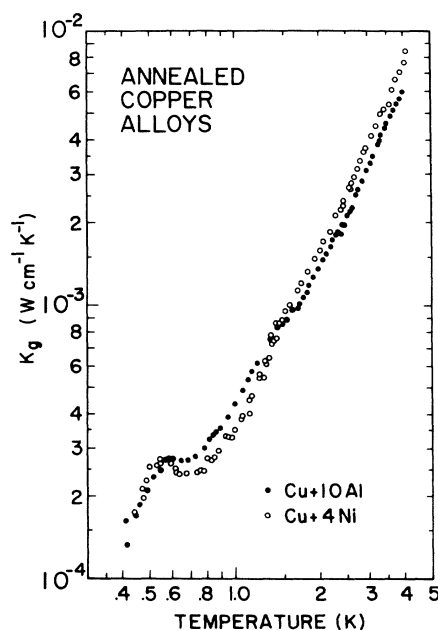


FIG. 8. K_g vs T for two annealed copper alloys.

compared in Fig. 8.

It seems plausible that in the annealed specimens the lattice conductivity below the secondary maximum is limited by phonon-electron scattering. From the values of K_g in that region one deduces a value of $W_g T^2$ of about $900 \text{ W}^{-1} \text{ cm K}^3$ for Cu-4-at. %Ni and $1100 \text{ W}^{-1} \text{ cm K}^3$ for Cu-10-at. %Al. This is not too different than the theoretical value for $W_{ge} T^2$ of $710 \text{ W}^{-1} \text{ cm K}^3$ of Eq. (8). Note that if the lattice thermal conductivity in the liquid- ^4He range (1-4 K) had been used to estimate $W_g T^2$, as has been done in a large number of earlier determinations, we would have obtained a higher value of $W_g T^2$.

It had already been suspected that these earlier, higher values of $W_g T^2$ of annealed alloys should not be identified with $W_{ge} T^2$, but perhaps contained resistance due to residual dislocations.^{45,46} A plot of $W_g T^2$ versus electron concentration, as in Fig. 9 and similar plots in Ref. 45, shows a cusp-like behavior near the parent metal, rather than the expected smooth dependence on electron concentration. Values of $W_g T^2$ deduced from our data near 4 K show the same anomalous behavior. Our values of $W_g T^2$ below 0.55 K are also shown: the dependence on electron concentration is now more regular.

While it was believed that the excess resistance could be due to dislocations, it was difficult to account for it in terms of sessile dislocations, as this would imply a very high residual dislocation density in the annealed alloys. If the excess re-

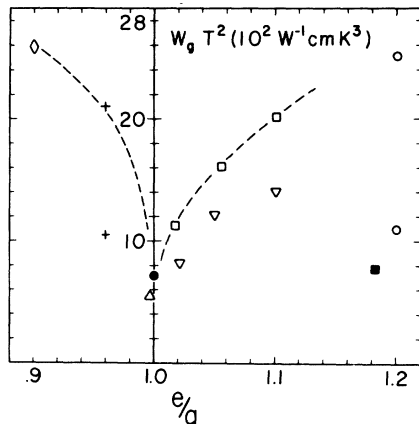


FIG. 9. $W_g T^2$ vs electron/atom ratio (after Kemp and Klemens, Ref. 45). \square , Cu-Zn annealed at 500°C ; ∇ , Cu-Zn annealed at 850°C ; Δ , Cu-Fe; \diamond , Cu-Ni. Our values: $+$, Cu-4-at. %Ni annealed at 1090°C , 60 h; \circ , Cu-10-at. %Al annealed at 1050°C , 60 h. \bullet , theoretical value for pure copper. For Cu-4-at. %Ni and Cu-10-at. %Al, the higher points are for $T \geq 3 \text{ K}$ and the lower points are for $T \leq 0.55 \text{ K}$. \blacksquare , Cu-6-at. %Ge (Jericho, Ref. 29). The dashed curves show the rapid increase in W_g , obtained by fitting K_g to a T^2 dependence at $T > 3 \text{ K}$.

sistance is ascribed rather to vibrating dislocations, this difficulty disappears. The fact that $W_g T^2$ below 0.55 K agrees well with the theoretical value of $W_{ge} T^2$ and with values of $W_g T^2$ for more dilute annealed alloys confirms this interpretation.

Lattice thermal conductivities of annealed silver alloys reported by Jericho²⁹ and data on a variety of alloys reported by Kapoor *et al.*²⁸ also support this interpretation. Thus, for Jericho's Ag-5-at. %Sb, $W_g T^2$ is $410 \text{ W}^{-1} \text{ cm K}^3$ below 1 K, in agreement with the theoretical value of $430 \text{ W}^{-1} \text{ cm K}^3$ for Ag of Eq. (8).

One difficulty with this interpretation is that according to the considerations of Pippard³¹ one would have expected W_{ge} to be strongly reduced below the values of (8) if the electron mean free path L_e is less than the dominant phonon wavelength λ , and K_g to decrease more slowly than T^2 with temperature. In Evanohm, L_e is around 10 \AA ; in the copper alloys it is about 100 \AA . Below 1 K, λ exceeds 1500 \AA , so that W_{ge} should indeed be strongly affected. This does not appear to be the case. Since the Pippard prediction is well founded theoretically, and generally confirmed at ultrasonic frequencies, the absence of such an effect in the present case is difficult to understand.

VI. SUMMARY

The effect of truncated dislocations predicted by Ackerman and Klemens¹³ were seen in deformed Evanohm. The effect may well be present also in the two deformed copper alloys, but cannot be clearly identified because it is overshadowed by an anomaly attributed to phonon scattering by mobile dislocations. This latter scattering has resonance character, and is also present in the annealed copper alloy specimens. Since the apparent resonance frequency seems independent of dislocation density and the same for both copper alloys, the resonance is probably associated with the Peierls potential. Were it not for the strong scattering of phonons by residual dislocations, the lattice thermal conductivity of annealed alloys would be a regular function of electron concentration.

ACKNOWLEDGMENTS

The authors wish to thank Dr. D. H. Damon and Dr. N. Louat for their continuing assistance throughout this work, and Dr. S. B. Woods, Dr. J. A. Rowlands, and Dr. A. Kapoor of the University of Alberta for their cooperation in providing us with their results prior to publication. We also thank the Wilbur B. Driver Co. for supplying the Evanohm samples, and P. Saunders, P. Smith, H. Taylor, and Miss L. Harrington for technical assistance. Helium for this work was provided by the U. S. Office of Naval Research, under Con-

tract No. 4500/N000 14-71-C-0249. Data reduction was accomplished using the facilities of the University of Connecticut Computer Center under

NSF Grant No. GJ-9. This work was initiated under the late C. A. Reynolds and the authors gratefully acknowledge his contributions.

- *Work supported by U. S. Air Force Office of Scientific Research under Project Themis and under Grant No. AFOSR-73-2418.
- †Present address: Materials Science Div., Argonne National Laboratory, Argonne, Ill. 60439.
- ¹P. Lindenfeld and W. B. Pennebaker, *Phys. Rev.* **127**, 1881 (1962).
- ²J. E. Zimmerman, *J. Phys. Chem. Solids* **11**, 299 (1959).
- ³M. A. Mitchell, P. G. Klemens, and C. A. Reynolds, *Phys. Rev. B* **3**, 1119 (1971).
- ⁴A. J. Friedman, T. K. Chu, P. G. Klemens, and C. A. Reynolds, *Phys. Rev. B* **6**, 356 (1972).
- ⁵A. J. Friedman, *Phys. Rev. B* **7**, 663 (1973).
- ⁶A. D. W. Leaver and P. Charsley, *J. Phys. F* **1**, 28 (1971).
- ⁷M. S. R. Chari and J. de Nobel, *Physica (Utr.)* **25**, 84 (1959).
- ⁸M. Kusunoki and H. Suzuki, *J. Phys. Soc. Jpn.* **26**, 932 (1969).
- ⁹J. A. Rowlands, A. Kapoor, and S. B. Woods, in *Proceedings of the Thirteenth International Conference on Low Temperature Physics, Boulder, Colo.*, 1972, edited by R. H. Kropschot and K. D. Timmerhaus (University of Colorado Press, Boulder, Colo., 1973).
- ¹⁰R. E. B. Makinson, *Proc. Camb. Philos. Soc.* **34**, 474 (1938).
- ¹¹P. G. Klemens, in *Handbuch der Physik*, edited by S. Flügge (Springer, Berlin, 1956), Vol. 14.
- ¹²P. G. Klemens, in *Solid State Physics*, edited by F. Seitz and D. Turnbull (Academic, New York, 1958), Vol. 7.
- ¹³M. W. Ackerman and P. G. Klemens, *Phys. Rev. B* **3**, 2375 (1971).
- ¹⁴Evanohm is a trademark of the Wilbur D. Driver Co., 1875 McCarter Highway, Newark, N. J.
- ¹⁵Materials Research Corp., Orangeburg, N. Y.
- ¹⁶P. Lindenfeld and W. B. Pennebaker, *Proceedings of the Seventh International Conference on Low Temperature Physics, Toronto, Canada*, 1960, edited by G. M. Graham and A. C. Hollis Hallett (University of Toronto Press, Toronto, 1961).
- ¹⁷F. W. Young, Jr. and J. R. Savage, *J. Appl. Phys.* **35**, 1917 (1964).
- ¹⁸J. E. Gueths, N. N. Clark, D. Markowitz, F. V. Burckbuchler, and C. A. Reynolds, *Phys. Rev.* **163**, 364 (1967).
- ¹⁹T. K. Chu and F. P. Lipschultz, *J. Appl. Phys.* **43**, 2505 (1972).
- ²⁰M. C. Karamargin, C. A. Reynolds, F. P. Lipschultz, and P. G. Klemens, *Phys. Rev. B* **5**, 2856 (1972).
- ²¹Janis Research Co., Stoneham, Mass.
- ²²R. J. Linz, Ph.D. thesis (University of Connecticut, 1973) (unpublished).
- ²³D. J. Strom and R. J. Linz, *J. Appl. Phys.* **44**, 917 (1973).
- ²⁴F. V. Burckbuchler and C. A. Reynolds, *Phys. Rev.* **175**, 550 (1968).
- ²⁵E. Lerner and J. G. Daunt, *Rev. Sci. Instrum.* **35**, 1069 (1964); R. C. Pandorf, E. Lerner and J. G. Daunt, *ibid.* **35**, 1070 (1964).
- ²⁶A. N. Gerritsen, in *Handbuch der Physik*, edited by S. Flügge (Springer, Berlin, 1956), Vol. 19.
- ²⁷C. G. Robbins, H. Claus, and P. A. Beck, *Phys. Rev. Lett.* **22**, 1307 (1969).
- ²⁸A. Kapoor, J. A. Rowlands, and S. B. Woods, *Phys. Rev. B* **9**, 1223 (1974).
- ²⁹M. H. Jericho, *Philos. Trans. Roy. Soc. Lond. A* **257**, 385 (1965).
- ³⁰P. G. Klemens, *Austr. J. Phys.* **7**, 57 (1954).
- ³¹A. B. Pippard, *Philos. Mag.* **46**, 1104 (1955); *J. Phys. Chem. Solids* **3**, 175 (1957).
- ³²M. W. Ackerman, *Phys. Rev. B* **5**, 2751 (1972).
- ³³P. Grüner and H. Bross, *Phys. Rev.* **172**, 583 (1968).
- ³⁴J. M. Ziman, *Electrons and Phonons* (Oxford U. P., Oxford, 1970).
- ³⁵A. Granato and K. Lücke, *J. Appl. Phys.* **27**, 583 (1956); **27**, 789 (1956).
- ³⁶A. C. Anderson and M. E. Malinowski, *Phys. Rev. B* **5**, 3199 (1972).
- ³⁷S. G. O'Hara and A. C. Anderson, *Phys. Rev. B* **9**, 3730 (1974).
- ³⁸A. C. Anderson and S. C. Smith, *J. Phys. Chem. Solids* **34**, 111 (1973).
- ³⁹H. Kronmüller, *Phys. Status Solidi B* **52**, 231 (1972).
- ⁴⁰See, for example, J. Friedel, *Dislocations* (Pergamon, Oxford, 1964).
- ⁴¹M. W. Ackerman and P. G. Klemens, *J. Appl. Phys.* **39**, 968 (1971).
- ⁴²P. C. J. Gallagher, *Metall. Trans.* **1**, 2429 (1970).
- ⁴³I. R. Harris, I. L. Dillamore, R. E. Smallman, and B. E. P. Beeston, *Philos. Mag.* **14**, 325 (1966).
- ⁴⁴J. W. Mitchell, J. C. Chevrier, B. J. Hockey, and J. P. Monaghan, Jr., *Can. J. Phys.* **45**, 453 (1967).
- ⁴⁵W. R. G. Kemp and P. G. Klemens, *Aust. J. Phys.* **13**, 247 (1960).
- ⁴⁶P. G. Klemens, in *Thermal Conductivity*, edited by R. P. Tye (Academic, New York, 1969).